

N O T I C E

THIS DOCUMENT HAS BEEN REPRODUCED FROM
MICROFICHE. ALTHOUGH IT IS RECOGNIZED THAT
CERTAIN PORTIONS ARE ILLEGIBLE, IT IS BEING RELEASED
IN THE INTEREST OF MAKING AVAILABLE AS MUCH
INFORMATION AS POSSIBLE

"Made available under NASA sponsorship
in the interest of early and wide dis-
semination of Earth Resources Survey
Program information and without liability
for any use made thereof."

NCC 5-22

80-10312
CR-163401

An Investigation of Vegetation and Other Earth
Resource/Feature Parameters Using Landsat and Other Remote
Sensing Data

I. Landsat

II. Remote Sensing of Volcanic Emissions

Semi-Annual Status Report (#1)

February 1 to July 31, 1980

Original photography may be purchased from
EROS Data Center

Dartmouth College

Sioux Falls, SD, 57198

Hanover, NH 03755

Principal Investigators:

Richard W. Birnie, Professor of Geology

Richard E. Stoiber, Emeritus Professor of Geology

Researchers:

Emily Bryant, Senior Research Assistant

A. G. Dodge, Area Forester Cooperative Extension Service (UNH)

Ken Sutherland, Assistant Grafton County Forester (UNH)

Joseph Francica, graduate student

John Hughes, graduate student

Lawrence Malinconico, graduate student

Stanley Williams, graduate student

Undergraduate Student Assistants

(E80-10312) AN INVESTIGATION OF VEGETATION
AND OTHER EARTH RESOURCE/FEATURE PARAMETERS
USING LANDSAT AND OTHER REMOTE SENSING DATA.
1: LANDSAT. 2: REMOTE SENSING OF VOLCANIC
EMISSIONS Semianual Status (Dartmouth

N80-32807

Unclassified
G3/43 00312

Dartmouth College

Semi-Annual Status Report - NCC 5-22

February 1, 1980 - July 31, 1980

This report covers activities of the Landsat Sensing Research Group (Earth Resources) and of the Volcanic Gas Sensing Research Group (Planetary Science) which work in collaboration with the Goddard Institute for Space Studies, New York; Dr. Robert Jastrow, Director. Dr. Stephen Ungar of GISS is the Technical Officer for this project.

NCC 5-22 supports work which was started in 1974 under NSG 5014.

I. Landsat

The Dartmouth Landsat Research Group continued application studies for Landsat data under the general category of analysis of vegetation cover, especially forestry and geobotany, that is, the effects of soil/earth mineral content on vegetation.

A. Forestry. The forestry group has had the same three permanent people working as in the previous year: Emily Bryant, Ken Sutherland, and Gibb Dodge. They were ably assisted by three undergraduates: John Stix, Dan Goodwin, and Dave Crampton.

Our efforts lay in three general areas: Landsat classification research, software use and development, and spreading the word/contact with others.

1. Classification Research

a. John Stix and Em initiated a study of the use of the GISS fan algorithm in classification of forest types. The fan algorithm is used to classify a landscape consisting of a continuum

between two pure cover types. In this case the continuum ranges from pure hardwood to pure softwood forest types. The fan algorithm places pixels in subcategories based on where their reflected radiance lies with respect to the signatures of the pure types. We wish to investigate the relationship between the fan subcategory that a pixel is placed in and the actual percent mixture of pure types found in the corresponding area on the ground.

We have done background work on learning how to use the fan algorithm, getting the programs to run, and setting up the initial supervised classification from which the fan will select categories. When this is done, we will apply the classification to the Ashland District in northern Maine, an area which was classified previously in the Seven Islands project.

b. Dave Crampton pursued the "fudge factor" question (temporal signature extension) using data from July and August of 1976 covering the Ashland District in Maine. Using five sets of training sites, he made five estimates of a correction function (the "fudge factor"). It was applied to the July data as compensation for atmospheric and other differences so that signatures used previously on the August data could be used on the July data as well.

Preliminary results from classification of one township in the district show that the acreages of forest types in the July map differ from the August map by 1.2% to 28% depending on the forest type and the correction function used. The function which was derived from all five sets of training sites combined gave acreage differences of -5.8% (softwood), +3.4% (mixed wood), and -4.7% (hardwood). Further tests will be made using other estimates of

the function and applying it to another township.

2. Software Development and Use.

a. Dan Goodwin made trial runs of the various supervised and unsupervised classification algorithms in the ISURSL programs on two areas of interest to the forestry group: Concord, NH, and part of the Ashland District in Maine. The object was to become familiar with the programs, compare classification results with those from the GISS algorithm, and to identify the strong and weak points of the programs.

He found use of the programs quite straightforward. Classification results compared well with the GISS algorithm--acreages for forest types on the Ashland district area were brought to within 4.8% of a classification done using the GISS algorithm. Strong points in the ISURSL programs included a useful data display in the histogram program, the capability of running many training sites at a time to determine signatures, and the use of one of the programs for one-band density slicing (a kind of hand-made gray scale). Limitations encountered were that all jobs must be run from tape, there is no polygon masking program available, and that some of the statistics which are useful come with voluminous others which are not as useful and cannot be turned off.

We conclude from this project that classification results are dependent as much or more on the familiarity of the user with whatever algorithm is being used as on the inherent attributes of the algorithm.

b. Dan Goodwin also wrote programs to rotate classification map output, for instance, for the user who wants his digital

Landsat map to have north be vertical on the page. These were written on both the Dartmouth and the GISS computers. The version on the GISS computer can handle a certain amount of scale change and change of symbols as well as rotation.

c. Em wrote a program called DELTAS on the Dartmouth computer which helps the user choose classification parameters for the GISS algorithm. It displays training site data in "difference space" (rather than color space), making it easier to predict the effect that a change in classification parameters will have on classification results. The DELTAS program was applied to development of forest type signatures for the Ashland District. Comparison with accounts of an earlier effort at making signatures for the same area showed that the DELTAS program helped increase efficiency in signature development.

d. Em wrote a program called ACCRACY on the Dartmouth computer. It displays a classification map with corresponding digital ground truth and prints a confusion matrix for the two.

e. Signature packages which have been developed for forest types on various Landsat passes over the past five years were typed into the file EFESB.SIGPACK which is accessible through GISS/Wylbur. Any Wylbur user can use the signatures by copying them into a GISS classification program.

3. Spreading the Word.

a. The manuscript on the Seven Islands project was revised and was accepted by the journal Photogrammetric Engineering and Remote Sensing. (Abstract, Enclosure 1. A reprint will be included in a future report.)

b. Landsat maps were given to John Ricard for field testing by local forest fire officials this summer.

c. Help was given to students in Earth Sciences 32 (remote sensing) in winter term with use of GISS hardware and software.

d. Em gave a lecture on digital Landsat data classification to Dave Lindgren's (Geography) remote sensing class.

e. Gibb and Em went to New York to talk over research plans with GISS personnel.

f. Dartmouth remote sensing meetings have continued on the average of once a month. Sam Goward (Columbia) gave a guest talk in January.

g. Maps of the White Mountain National Forest were presented to Forest Service personnel at their headquarters in Laconia, NH, by Gibb, Ken, and Em. Their preliminary reaction was that this type of information could be used better on a general level than on their local level, but we still await a more detailed reaction.

h. Gibb, Ken, and Em attended a meeting organized by the New Hampshire State Office of Comprehensive Planning to investigate the possibility of setting up an ERRSAC Landsat Demonstration Project in New Hampshire.

4. Other items.

We have had a fair number of hardware problems this half-year. The Cope card reader was down for a couple of week-long periods.

Em will be entering the two-year Dartmouth Master's program in Computer and Information Science as a student in September and

will be working half-time instead of full-time starting then.

The progress report, furnished under the terms of the Dartmouth Task Order to UNH, for the period October 31, 1979 - May 1, 1980 is at Enclosure 2.

B. Geology and Geobotany. The geologic remote sensing group has worked in three major areas over the last six months.

1. The project on the geologic mapping of the Landsat data has been completed. A Master's thesis was submitted by Joseph Francica (June 1980) (Enclosure 3) and a paper was presented at the 14th annual ERIM symposium in Costa Rica (Francica, Birnie, and Johnson, 1980) (Enclosure 4). The project produced a series of 1:100,000 geologic maps interpreted from Landsat data. The maps cover over 11,600 square kilometers of the Ladakh Himalaya of Arabia and Pakistan. Landsat remote sensing techniques are nicely suited to this area because the high relief and limited accessibility make conventional geologic mapping very difficult and the dearth of vegetation and absence of atmospheric haze make clear bedrock exposures for the satellite.

2. A project was undertaken using Landsat data to identify and map lateral spectral contrasts in the Lower Hudson River Estuary. These lateral spectral contrasts were detected using the supervised classification algorithm developed at GISS. The analysis of Landsat data lead us to conclude that there is a relatively strong downstream flow on the west side of the river and that the western water is more turbid and less saline than the eastern water. These results were presented at the 14th annual ERIM Symposium in Costa Rica (Birnie and Posmentier, 1980) (Enclosure 5).

3. The third project involves our ongoing program to use airborne multispectral scanner data to detect geobotanical anomalies associated with mineralized ground. Data from the Mesatchee Creek experiment has been reevaluated and a paper has been revised and resubmitted to Economic Geology (Enclosure 6). At Mesatchee Creek, a strong geobotanical anomaly was detected and was determined to correlate with the pyrite halo of a porphyry copper deposit.

4. John Hughes wrote a number of programs for use with LANDSAT Digital Data on the Dartmouth Computer (Enclosure 7).

II. Remote Sensing of Volcanic Emissions

The principal activities of this group (Professor Richard E. Stoiber and Graduate Students Lawrence Malinconico and Stanley Williams) during this period (February - July 1980) were concerned with preparations, field work, and reports for visits to Guatemala and to Washington state (Mt. St. Helens). (Work in Nicaragua in February and August 1980 is related to this effort but is funded by the NSF.)

1. Guatemala. February 4 - 18, 1980. Stoiber, Malinconico, Williams.

Our group was associated with the NCAR volcanic plume project in Guatemala. We flew through the gas of eruptive columns and beneath and through horizontal volcanic plumes. SO₂ output was measured with the airborne COSPEC. Excellent data were obtained from two volcanoes: Santiaguito and Feugo, (and some data from Pacaya). It is being processed. An important feature of this project was that data were obtained by other scientists as to gas

composition and particulates. This was done at the same time as, and in coordination with, the SO₂ measurements. A discussion of the results is planned in Denver in late May. We will contribute.

The new data collected chiefly concerned the configuration of the volcanic plumes, both in vertical and two horizontal dimension. Analyses such as these have not hitherto been made.

Also, see Enclosure 10, below, for discussion of review session.

2. Mt. St. Helens. March 28 - April 6, 1980, April 9 - 13, 1980, May 18 - 26, 1980, July 2 - 9, 1980. Stoiber, Williams, Malinconico.

A major series of ventings and eruptions from Mt. St. Helens over a period of several months (continuing) provided unique opportunities to test and employ the COSPEC in an operational role.

Four field trips, which were partially supported by NCC 5-22, are described in Enclosures 8, 9, 10, and 11.

A fortunate confluence of interest with NBC news provided free use of an airplane for airborne monitoring and national publicity for the efforts and expertise of Professor Stoiber.

In addition, the data obtained in the period March 28 - April 13, 1980, became the basis for an article submitted to SCIENCE on April 17, 1980 and published on June 13, 1980 (Enclosure 12).

As reported in Enclosure 10, the Dartmouth-NASA COSPEC was loaned to the USGS on April 13, for use by them in continuous monitoring of Mt. St. Helens (until a USGS COSPEC could be made available.) Unfortunately, the scientist who was using the COSPEC was killed in the direct blast of the May 18 eruption and the COSPEC was destroyed, or at least buried irretrievably. Insurance coverage

of the COSPEC (a common practice in field work using expensive instruments) provided funds for immediate replacement of the COSPEC, for use in subsequent work in Nicaragua.

3. Nicaragua. February 1980, July - August 1980. Stoiber, Williams, Malinconico.

This work, supported by the NSF, involves monitoring of the plumes of volcanoes Masaya and San Cristobal and generally helps develop our expertise in this field.

Enclosures 1 - 12 a/s.

11

Landsat for Practical Forest Type Mapping

A Test Case

Emily Dryant

Arthur G. Dodge, Jr.

Samuel D. Warren

Abstract: In a cooperative project, computer classified Landsat maps were compared with a recent inventory of forest lands in northern Maine. Over the 196,000 hectare (485,000 acre) area mapped, estimates of area of softwood, mixed wood, and hardwood forest types by the two methods agreed to within 5%. Cost of the Landsat maps is estimated at 6.5 cents per hectare (2.6 cents per acre). Although the information derived from Landsat is not yet refined enough to be incorporated in current forest inventories, the techniques used are worth developing.

(Revised manuscript submitted
to Photogrammetric Engineering
and Remote Sensing, April 1980)

Encl 1

PROGRESS REPORT

APPLYING LANDSAT MEASUREMENTS TO FOREST RESOURCE INVENTORIES

October 31, 1979 - May 1, 1980

Ken Sutherland and Gibb Dodge, Cooperative Extension Service, coordinated their activities with Emily Bryant, Dartmouth College, and other representatives of GISS.

Site Selection

1. Finished developing field maps of Groveton Papers (Diamond International) test compartment. Will deliver to the company and test usefulness.
2. Assisted in developing criteria and categories for mapping White Mountain National Forest by districts. Met with WMNF Staff to obtain input on maps developed.
3. Developed map of the town of Plymouth for use by New Hampshire Forest Fire Service which was put into the hands of local fire suppression personnel for test use.

Guidance and Evaluation

1. Guidance to:
 - a) GISS on making changes in computer programs to produce better output products (polygon, legend, scale change, line, smoothing, etc.) continued.
 - b) Dartmouth work-study students - mapping techniques, observing ground truth sites, development of rotation and scale change program.
 - c) N.H. Forest Fire Service - using computer maps as field tools.
 - d) Revise and update 1980 work plans.
2. Evaluation:
 - a) Analyze computer outputs resulting from GISS program changes.
 - b) Changes indicated on Landsat maps by comparing 1975 and 1978 data.
 - c) New rotation and scale changing program.

Collaboration

1. Serving on Cooperative Extension Service National Task Force for remote sensing - advice to Extension Committee on policy related to Extension activity in remote sensing technology transfer.
2. Update information to the University of Vermont, University of New Hampshire, Maine Forestry Planning Group, GISS, ERRSAC, GSFC, Remote Sensing Group of Northern

New England, New Hampshire Fish and Game Department and Office of State Planning.

3. Remote sensing meetings with New Hampshire Office of State Planning, University of New Hampshire and Dartmouth.

4. Met with N.H. Office of State Planning personnel on New Hampshire Landsat demonstration project with ERRSAC.

Technology Transfer and Reporting

1. Landsat presentations to classes at Dartmouth.
2. Generate remote sensing technology to New Hampshire Fish and Game Department and Division of Forests and Lands.
3. Co-sponsor remote sensing workshop for State agencies with Office of State Planning.

Submitted by,

Kenneth I. Sutherland, Jr.,
Program Assistant

Arthur G. Dodge, Jr.,
Program Leader

14

GEOLOGIC MAPPING OF THE LADAKH HIMALAYA
BY COMPUTER PROCESSING OF LANDSAT DATA

A Thesis
Submitted to the Faculty
in partial fulfillment of the requirements for the
degree of
Master of Arts

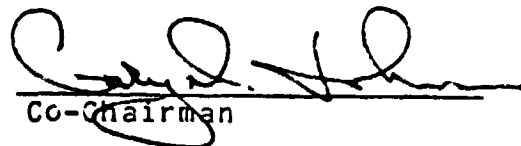
by
Joseph R. Francica, Jr.

DARTMOUTH COLLEGE
Hanover, New Hampshire
June 1980

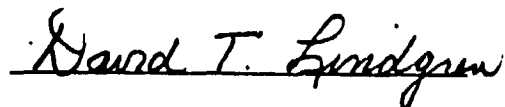
ORIGINAL PAGE IS
OF POOR QUALITY

Examining Committee:


Richard E. Francica
Co-Chairman


Charles L. Drury
Co-Chairman


Charles L. Drury
Dean of Graduate Studies


David T. Lundgren

Encl 3

ABSTRACT

Computer processed Landsat digital data were used to map the geology of 11,600 square kilometers of the Ladakh Himalaya of India and Pakistan. The results of a supervised classification algorithm were integrated with field studies to produce 1:100,000 geologic maps of this area. Six major rock types have been discriminated by Landsat data and were mapped. High relief and limited accessibility of the terrain make conventional geologic mapping difficult. This region was particularly suited for a Landsat data analysis, however, because the bedrock geology is clearly exposed as a result of the dearth of vegetation and the absence of atmospheric haze.

16

Proc. 14th Int. Symp. Remote
Sensing of Environment
23-30 April, 1980,
San Jose, Costa Rica (in press)

GEOLOGIC MAPPING OF THE LADAKH HIMALAYA
BY COMPUTER PROCESSING OF LANDSAT DATA

Joseph R. Francica, Richard W. Birnie, and Gary D. Johnson

Dept. of Earth Sciences
Dartmouth College
Hanover, NH 03755

ABSTRACT

Computer processed Landsat digital data and field studies have been integrated to make a geologic map of the Indus Suture in the Ladakh Himalaya. This co-ordinated approach has been successful at locating and identifying the areal extent of the major rock bodies in a 2500 square kilometer area, much of which is inaccessible for conventional field geologic studies.

1. INTRODUCTION

Landsat digital data have been used to make a geologic map of portions of the Ladakh Himalaya of northern India and Pakistan. The study area encompasses the Indus suture, a tectonically complex zone of regional geologic importance. This region is particularly suited to Landsat-based analysis because of the clear exposure of the surface geology resulting from the paucity of vegetation and the absence of atmospheric haze. The high relief and limited accessibility of the terrain make geologic mapping by conventional techniques difficult.

Approximately 12,000 square kilometers of terrain are being mapped; however, only two representative regions totalling about 2500 square kilometers are presented here: 1) the Kargil region in the western limit of the study area, and 2) the Leh region in the eastern limit of the study area (Fig. 1). These regions are illustrative of our techniques and exhibit the major problems in the definition of rock body boundaries.

2. GEOLOGY

The Indus suture, interpreted as a tectonic boundary between zones of varying rock type and petrogenesis (Heim and Gansser, 1939; Gansser, 1964, 1974, 1977, 1980; Powell and Conaghan, 1973 and 1975; Crawford, 1974) is characterized in the Kargil-Leh area as a zone of three to four narrow, steeply thrust sheets of ophiolitic melange with associated ultramafic rocks (Frank et al., 1977). The ophiolitic melange and ultramafics, although well exposed and easily mapped in certain regions of the Kargil-Leh area, do not have

1

ORIGINAL PAGE IS
OF POOR QUALITY

Encl 4

19

sufficient exposure to be mapped in the regions reported herein. The rock units associated with the Indus Suture and mapped in this study are described below.

The Dras Volcanics (Wadia, 1937) are principally composed of metamorphosed augite andesites, hornblende andesites and basalts (Frank et al., 1977). In the eastern portion of the study area, this unit grades into volcanoclastic and interbedded metasediments. Gupta et al., (1975) have established a Cretaceous age for this unit.

The Ladakh Intrusives (Frank et al., 1977) have the largest areal extent of any rock unit within the study area. Generally, they vary in composition from granite to granodiorite in composition. Near Kargil, the intrusives include a suite of norites, gabbros and diorites. To the east near Leh, small diorite stocks and diabasic dikes are present. The intrusives are Cretaceous to Tertiary in age (Frank et al., 1977; Shah et al., 1976).

The Ladakh Molasse (Tewari, 1964) separates the Ladakh granites to the north from the Dras Volcanics to the south. This late orogenic, primarily fluvial, clastic sequence is composed of intercalated channel sandstones and overbank mudstone lithofacies.

The Indus Flysch (Frank et al., 1977) consists of thinly bedded, fissile shales and sandstones. An early Mesozoic age is suggested for these rocks (Tewari, 1964, Frank et al., 1977).

Unconsolidated Quaternary deposits abound in the Kargil-Leh area.

3. LANDSAT DATA ANALYSIS

The geocorrected Landsat digital data (Scene E-30135-04495) were classified according to a supervised classification scheme developed by S. Ungar at NASA's Goddard Institute for Space Studies (Merry et al., 1977). This same classification scheme has been applied to a study of the Hudson River Estuary (Birnie and Posmentier, this volume) where the following description is repeated. In this classification scheme, a surface type is assigned a vector signature whose components are the four individual Landsat band values. The spectral distance from this signature to a pixel to be classified is calculated and tested for acceptability relative to the user specified maximum allowable distance (DELMAX). This dimensionless distance is based on two factors: color difference (ΔC) and brightness difference (ΔB).

To calculate the color difference (ΔC), the vectors in Landsat color space corresponding to the signature and pixel to be classified are normalized to unit length. The ΔC is the chord length between the tips of the signature and pixel unit vectors.

The brightness of a pixel is determined by summing the four individual band reflected radiance values. The brightness difference (ΔB) between a pixel and signature is defined as the absolute value of their difference in brightness divided by their average brightness.

The overall distance (D) between a pixel and a signature is calculated by the following relationship where the user chooses the degree to which color differences (ΔC) and brightness differences (ΔB) are to be weighted (WCLR and WBRT respectively):

$$D = \sqrt{WCLR \cdot (\Delta C)^2 + WBRT \cdot (\Delta B)^2}$$

where $WBRT + WCLR = 1$.

If the distance D is less than a user-specified value (DELMAX), then the unknown pixel will be classified as belonging to the surface type associated with that signature.

A four-dimensional classification volume is described about each signature. The shape and orientation of the volume changes depending on the values of WBRT, WCLR, and DELMAX, but is generalized as a distorted hyper-ellipsoid inscribed within a truncated cone.

Training sites of known geologic units were selected on the basis of field work and published reconnaissance maps of the area. Spectral signatures for each unit were determined by averaging all pixels within a training site. Values of WBRT, WCLR, and DELMAX for each signature were optimized by choosing those values that minimized the sum of the errors of omission and commission of each training site compared to all other training sites.

The classification scheme is order dependant. Pixels which fall in more than one classification volume are classified as the first one tested. For example, areas of alluvium often classify as a granite because their volumes overlap and granite is classified before alluvium. A knowledge of which surface types created the overlap problems was used to set up the classification hierarchy and interpret the results.

Before field investigations were undertaken in August and September of 1979, a preliminary map was generated for the Kargil region (Fig. 1). This area contains rock types representative of the Kargil-Leh area as a whole. The town of Kargil served as a base of operations from which other parts of the area were accessible. Most of the training sites on which the signatures are based are located in this region.

During the field investigations, training sites were studied in order to 1) confirm their geology and 2) identify the problems causing incorrect classifications. The accuracy of the classification of geologic units outside the training sites was also studied at this time. These new observations led to the selection of new training sites, and a refined and improved version of the preliminary classification map was made (Figures 2 and 4).

The large white areas represent unclassified pixels which, on the basis of geomorphology, we interpret to be shadowed. In these shadowed regions, the surface reflected radiance reaching Landsat is overwhelmed by backscattered path radiance. The different reflectivity properties of various surface materials are thus masked. Even though the Landsat data for Scene E-30135-04495 (July 18, 1978) were chosen to minimize the shadow problems (sun elevation = 58 degrees), the severe relief in the region results in extensive shadowing.

A geologic interpretation of the Landsat classification map was made by combining information in the classification map with field observations, geomorphic interpretations of 1:500,000 Landsat color composite imagery, and previously published geologic maps (refer to maps in Tewari, 1964; Shah et al., 1976; Frank et al., 1977).

4. DISCUSSION

4.1 The Kargil Region

The Dras Volcanics and the undifferentiated mafics of the Ladakh Intrusives have similar spectral signatures, respectively (Band 1 through Band 4 reflected radiance values in $\text{mw} \cdot \text{cm}^{-2} \cdot \text{sr}^{-1} \cdot \text{ch}^{-1}$: Dras Volcanics = .607, .596, .508, 1.088; Mafics = .662, .596, .510, 1.127). Because the volcanics appear first in our classification scheme, numerous mafic intrusive pixels are erroneously classified as volcanics. This example of commission error is corrected

by our field-based observation that computer classified areas of volcanics lying north of the main volcanic belt and separated from it by other rock bodies must be interpreted as mafic intrusives and not Dras Volcanics.

The Kargil basin has been the site of fluvio-glacial and lacustrine sedimentation during the latest Tertiary and Quaternary. Geomorphic evolution of the Suru and Wakka river valleys during the Quaternary has resulted in the development of a complex of terraces carved into these basin-fill sediments and on certain of the underlying older terrain. These were recognized on Landsat prior to entering the field but their areal extent did not reconcile with the extant geologic maps. Upon field study, we determined that the Landsat classification accurately portrayed the distribution of this unit. The classification shown in Figure 3 illustrates this distribution.

Agricultural land, easily identified on Landsat color composite imagery and on our classification map, was included as alluvial deposits because these lands are confined to irrigatable alluvial soils.

The Boundary between the Dras Volcanics and the Ladakh Molasse, which is clearly defined in the Landsat classification as a major rock body boundary, has been interpreted by Tewari (1964) as a thrust placing volcanics over molasse. This thrust constitutes one of the imbricate faults associated with the Indus suture described above.

4.2 The Leh Region

The classification map for the Leh region shows clear outcrop patterns for both the molasse and the intrusives. Signatures used previously in the Kargil region for these units are applied here with equal success. A new signature was added for a molasse with a lower albedo. The molasse has undergone a facies change in this region and exhibits a different albedo when compared to the molasse of the Kargil region.

A new signature for undifferentiated mafics of the Ladakh Intrusives unsuccessfully defined this rock type. The spectral signature for the mafics is similar to the signature for molasse (Band 1 through Band 4 reflected radiance values in $\text{mw} \cdot \text{cm}^{-2} \cdot \text{sr}^{-1} \cdot \text{ch}^{-1}$: Mafics = .824, .768, .634, 1.321; Molasse = .792, .729, .625, 1.264). The correction for the commission error in this region is accomplished by locating computer classified areas of molasse within the Ladakh Intrusives that we interpret to be mafics.

The alluvial deposits in this region have the same spectral characteristics as the rock type from which they were derived. Alluvial fans south of the Indus River, derived from the darker molasse, classify as molasse. The same applies for fans derived from the Ladakh Intrusives north of the Indus. Their location and areal distribution are mapped by the interpretation of high oblique, ground-based photos whose orientations are known exactly.

5. CONCLUSIONS

The types of problems associated with the two test regions, Kargil and Leh, are common throughout the entire study area. Based on the criteria for interpretation applied to these regions, other regions of the Ladakh Himalaya and adjacent Baltistan are being mapped in the same way. It is significant that the signatures developed in the Kargil region were then successfully applied in the Leh and other regions of the Indus suture zone. This fact illustrates the application of computer processed Landsat digital data to geologic mapping of large areas. However, it should be emphasized that Landsat is no panacea. Only in conjunction with careful field observations can the problems associated with regional topography and geological complexities be resolved.

ACKNOWLEDGMENTS

Appreciation is extended to the personnel of Peshawar University, Delhi University, and Geological Survey of India (Kashmir Circle), and the Goddard

20

Institute for Space Studies (GISS) for their interest in and support of this research. R.A.K. Tahirkheli, I. Noor, R.G.H. Reynolds and S.K. Tandon contributed variously to the field aspects of this project. The field work has been conducted in part under a collaborative project between Peshawar University (Pakistan) and Dartmouth College. The Landsat data analysis was undertaken as part of a collaborative program between GISS and Dartmouth College. S. Ungar, E. Stroock, C. Baum, and C.H. Stoops contributed to the Landsat analysis. This research was supported by U.S. National Science Foundation Grant INT77-18362 and EAR78-03639, U.S. National Aeronautics and Space Administration grant NSG 5014, Peshawar University, and Dartmouth College.

REFERENCES

- Crawford, A.R., 1974, The Indus Suture Line, the Himalaya, Tibet and Gondwanaland: Geological Magazine, v. 111, p. 369-383.
- Frank, W., Gansser, A., Trommsdorff, V., 1977, Geological Observations in the Ladakh Area (Himalayas): Schweiz. Mineral. Petrogr. Mitt., 57, p. 89-113.
- Gansser, A., 1964, Geology of the Himalayas: London, Wiley-Interscience.
- , 1974, The Ophiolitic Melange, A World-wide Problem on the Tethyan Examples: Eclogae Geol. Helv., v. 67/3, p. 479-507.
- , 1977, The Great Suture Zone between the Himalaya and Tibet. A preliminary account: Coll. int. C.N.R.S. Paris 1976. Ecologie et Géologie du Himalaya.
- , 1980, The significance of the Himalayan Suture zone, Tectonophysics, v. 62, p. 37-52.
- Gupta, V.J., and S. Kumar, 1975, Geology of Ladakh, Lahaul, and Spiti Regions of Himalaya with special reference to the Stratigraphic position of Flysch deposits: Geol. Rundschau, Band 64, p. 540-563.
- Haim, A., and A. Gansser, 1939, Central Himalaya. Geological Observations of the Swiss Expedition, 1936. Denkschr. Schweiz. Naturforsch. Ges., v. 73(1), p. 245.
- Merry, C.J., H.L. McKim, S. Cooper, and S.G. Ungar, 1977, Preliminary analysis of water equivalent/snow characteristics using Landsat digital processing techniques: Proceedings of 1977 Eastern Snow Conference, Beltsville, Ontario, Canada.
- Powell, C.M.C. and P.J. Conaghan, 1973, Plate tectonics and the Himalayas, Earth and Planetary Science Letters, v. 20, no. 1, p. 1-12.
- , and , 1975, Tectonic models of the Tibetan plateau, Geology v. 3, no. 12, p. 727-731.
- Shah, S.K., L. Sharma, J.T. Gergan and C.S. Tara, 1976, Stratigraphy and Structure of the Western Part of the Indus Suture belt, Ladakh, Northwest Himalaya: Himalayan Geology, v. 6, Wadia Institute of Himalayan Geology, Dehradun, India, p. 534-556.
- Tewari, A.P., 1964, On the Upper Tertiary deposits of Ladakh Himalayas and correlation of various geotectonic units of Ladakh with those of the Kumaon-Tibet region: Geol. Congr. XXII Sess., Part XI, p. 37-58.
- Wadia, D., 1937, The Cretaceous volcanic series of Astor-Deosai, Dashmir, and its intrusions. Rec. of Geol. Surv. India, v. 72, part 2, p. 151-161.

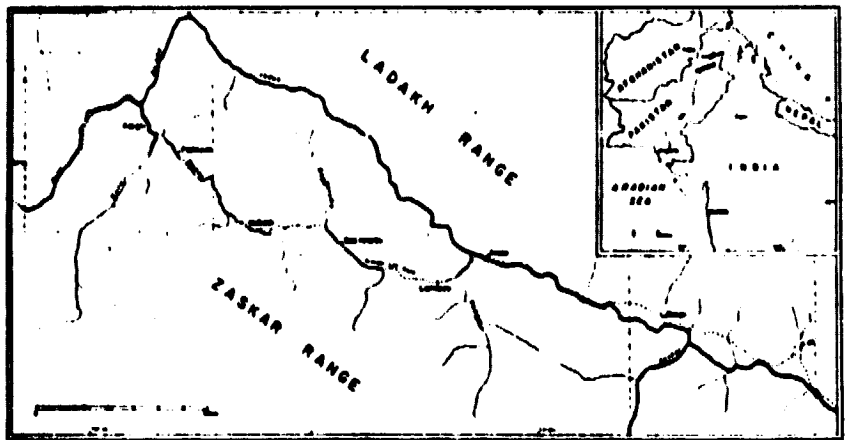


Figure 1. Study Area

Kargil and Leh regions on the west and east, respectively, are enclosed by dashed lines. Insert map shows the extent of Landsat scene E-30135-04495.

ORIGINAL COPY
OF POOR QUALITY

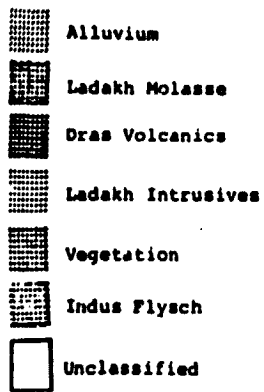


Figure 2. Landsat classification map for the Kargil region.
(For scale see Figure 3)

ORIGINAL PAGE IS
OF POOR QUALITY

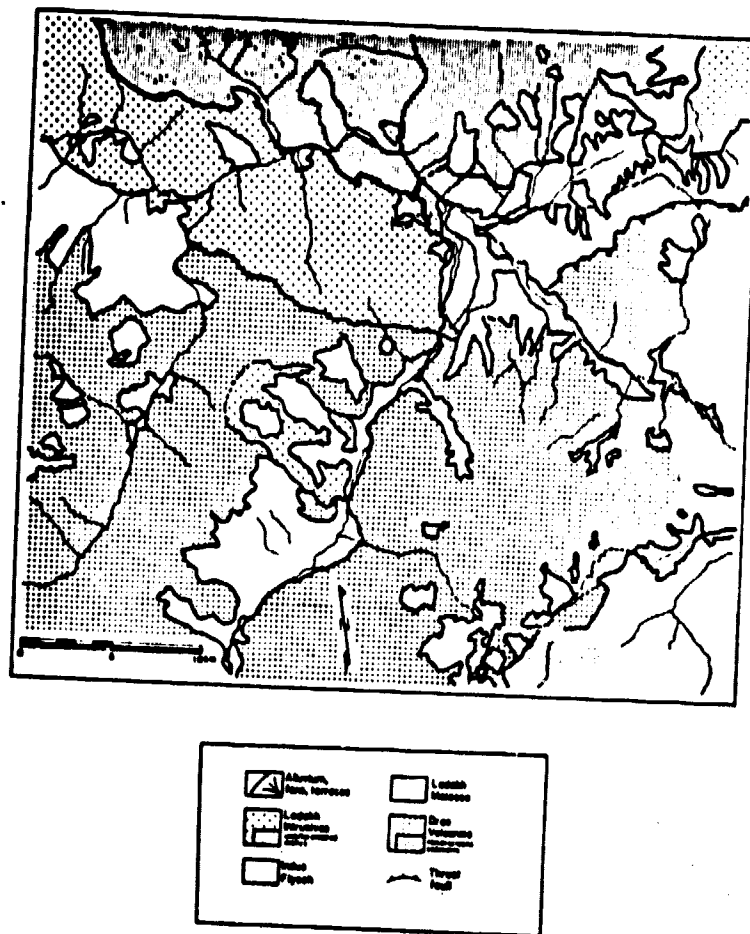


Figure 3. Geologic interpretation of the Kargil region classification map.

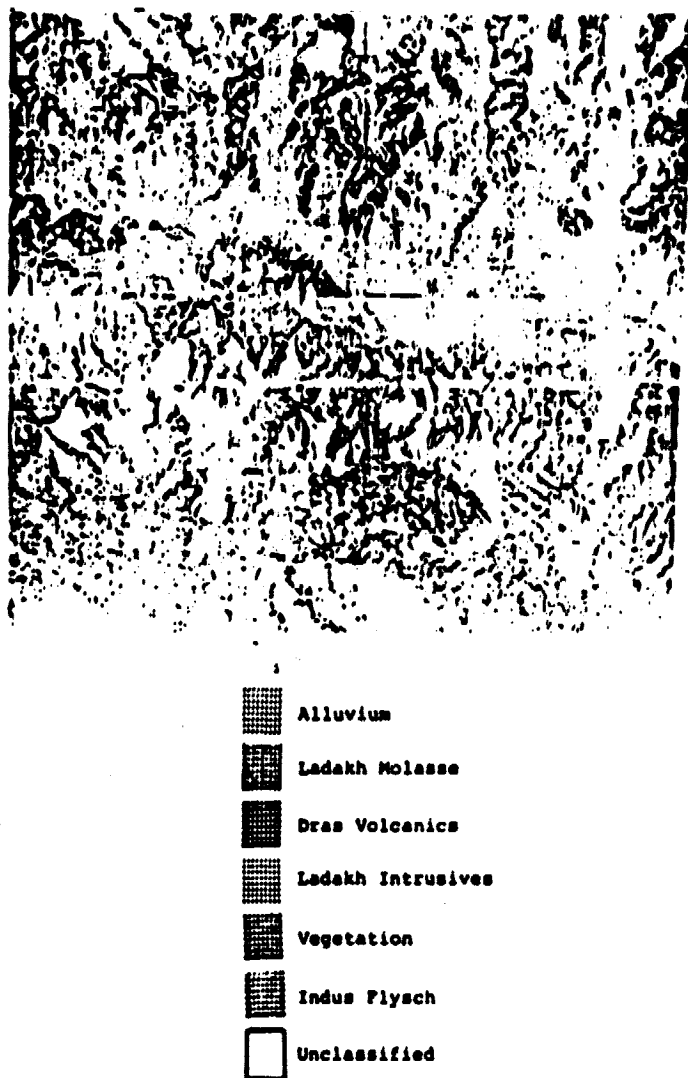


Figure 4. Landsat classification map for the Leh region.
(For scale see Figure 5)

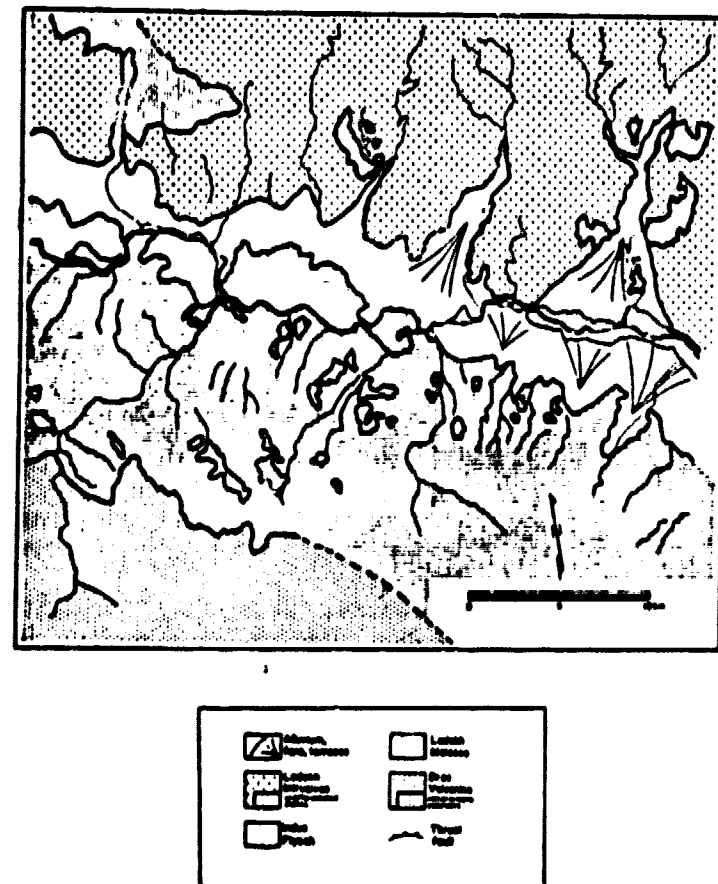


Figure 5. Geologic interpretation of the Leh region classification map.

ORIGINAL
FOR GOVERNMENT USE

26

Proc. 14th Int. Symp. Remote
Sensing of Environment
23-30 April, 1980
San Jose, Costa Rica (in press)

IDENTIFICATION OF LATERAL SPECTRAL CONTRASTS IN THE LOWER
HUDSON RIVER ESTUARY USING LANDSAT DIGITAL DATA

Richard W. Birnie
Dept. of Earth Sciences
Dartmouth College
Hanover, N.H. 03755

and

Eric S. Posmentier
Dept. of Earth Sciences
Dartmouth College
Hanover, N.H. 03755 and
Division of Natural Sciences
Southampton College of
Long Island University
Southampton, N.Y. 11968

ABSTRACT

An analysis of Landsat digital data has allowed us to detect and map lateral spectral contrasts in the Hudson River Estuary. These contrasts are believed to be related to turbidity in the Estuary with the western side being more turbid. It is clear that Landsat digital data can be mapped and used as an indicator of circulation and dispersion in the Hudson River Estuary.

1. INTRODUCTION

A study has been made of the Landsat digital data for the Lower Hudson River Estuary (Scene E-1096-15074, 27 Oct. 1972). The study area includes the region of the Upper Bay from 5 km south of the Verrazano Narrows up the river about 65 km to 5 km north of the Tappan Zee Bridge (Figure 1).

Initially, we are interested in confirming the presence of lateral gradients of water properties in the Hudson River Estuary to test whether there are processes that produce these lateral gradients at a rate sufficient to maintain them in the presence of lateral mixing. Until recently it has been assumed that there are no lateral gradients in the Hudson River Estuary, but recent observational and theoretical data (Posmentier and Reymont, 1979) support the presence of lateral gradients.

Secondly, if the lateral gradients exist, we are interested in determining whether they produce a sufficient spectral contrast over a large enough area to make them detectable and mappable using Landsat digital data.

2. PREVIOUS WORK

Other investigators have used remotely sensed surface reflectance and reflected radiance data to study coastal and estuarine waters. Applications of remote sensing techniques to coastal zone management have been summarized by Posmentier (1977). Rouse and Coleman (1976) correlated suspended sediment

Encl 5

concentration and reflected radiance in a laboratory experiment. They determined that a spectral band equivalent to Landsat MSS Band 3 (0.6-0.7 μ m) gave the best differentiation of suspended sediment levels. They assumed this correlation extended to actual Landsat data and used Band 3 imagery to study the circulation of the Louisiana Bight. Johnson and Bahn (1977) found significant correlations between reflectance in the 0.440-0.490 and 0.620-0.660 μ m bands of an airborne multispectral scanner and a number of water properties measured directly in the James River. These properties included suspended sediment, chlorophyll *a*, nitrite, nitrate, phosphate, salinity, and Secchi depth. Johnson (1978) found similar results for chlorophyll *a* and suspended sediment in the New York Bight. Khorram (1979) used four spectral bands (0.475-0.530, 0.550-0.610, 0.645-0.690, and 0.745-0.800 μ m) of an Ocean Color Scanner on a U-2 aircraft to estimate surface water electrical conductivity, chlorophyll concentration, suspended solids concentration, and turbidity. He was able to map these four water properties in the San Francisco Bay Delta. Klemas and Polis (1976) used Band 3 Landsat digital data and imagery to map suspended sediment concentration and tidal related variations in suspended sediment distribution patterns in the Delaware Bay. Landsat data were used to distinguish between seawater and freshwater, and among four classes of shallow marine and estuarine water categories near Cape Fear (Mausel et al., 1979). Mahees and Mausel (1979) delineated on the basis of Landsat data what they believed to be the salt wedge boundary in the Pamlico Estuary.

3. SALINITY DATA

As part of a physical oceanography and interdisciplinary study of the Hudson Estuary beginning in 1973, temperature, salinity, and conductivity were measured at cross-channel transects between the Apeas of the New York Bight to Saugerties, New York. Along each transect, from two to four stations were occupied; and the variables at each station were measured from the surface to the bottom. Temperature and salinity measurements were made with an Inter-Ocean probe with a manually-logged digital readout and an analog plotter on deck. The seasonal, longitudinal, and vertical distributions of salinity and temperature have been analyzed and are discussed by Posmentier and Rachlin (1976) and Posmentier and Raymont (1979).

The salinity data referred to in this paper were collected on 12-13 August, 1975, between 40°45' and 41°10' north latitude (Figures 1 and 2). The times of observation span four semidiurnal tidal cycles. Any small-scale salinity structure related to discontinuous point sources of seawater or freshwater would, therefore, be beyond the resolving capacity of the survey. Point-by-point comparison of the non-synoptic salinities with synoptic reflected radiance data would be meaningless unless the latter were available for precisely the same time as the salinity data. Since time correlative Landsat data were not available, it was decided to compare only the large-scale variations of salinity with those of the high quality Landsat scene of 27 October, 1972.

During the 12-13 August, 1975 Estuary study, there was very little temperature variability in the surface water. Therefore, only the salinity data, which were measured with an accuracy of 0.05‰, are presented in Figure 2. There were fourteen individual latitudinal transects. The distance from the shore to the ends of the transects was approximately 25% of the Estuary width. The west side surface salinities were less than those on the east (Figure 2). This indicates that there is a greater proportion of freshwater on the west. The average salinity difference was 0.749‰. An exception to the general trend occurred immediately south of the Piermont Pier (41°02' north latitude, Figure 1), where the higher salinity on the west might be due to the large horizontal eddy often observed on the wake of the pier which extends from the western shore one third of the way across the Estuary.

There are several factors which may contribute to the observed lateral salinity gradient in the Hudson Estuary. These include more freshwater runoff on the west side, the Coriolis effect on the net downstream surface flow, the internal Kelvin waves forced by tides in the ocean, the curvature of the Estuary axis, asymmetry in the Estuary cross section, and bottom friction. An evaluation of the hydrodynamic significance of these factors is beyond the scope of this paper, but it is in preparation for publication elsewhere. What is emphasized here is the interpretation that the higher salinity on the east side of the Estuary, whatever its cause, indicates a greater proportion of ocean water on the east side and a greater proportion of freshwater on the west side and confirms the presence of a lateral gradient of a water property.

4. LANDSAT DATA ANALYSIS

The geocorrected Landsat digital data (Scene E-1096-15074) were classified according to a supervised classification scheme developed by S. Ungar at NASA's Goddard Institute for Space Studies (Merry et al., 1977). This classification scheme has also been applied to a study of the distribution of rock types in the Ladakh Himalaya (Francica et al., this volume) where the following description is repeated. In this classification scheme, a surface type is assigned a vector signature whose components are the four individual Landsat Band values. The distance from this signature to a pixel to be classified is calculated and tested for acceptability relative to the user specified maximum allowable distance (DELMAX). This dimensionless distance is based on two factors: color difference (ΔC) and brightness difference (ΔB).

To calculate the color difference (ΔC), the vectors in Landsat color space corresponding to the signature and pixel to be classified are normalized to unit length. The ΔC is the chord length between the tips of the signature and pixel unit vectors.

The brightness of a pixel is determined by summing the four individual band reflected radiance values. The difference in brightness (ΔB) between a pixel and signature is defined as the absolute value of their difference in brightness divided by their average brightness.

The overall distance (D) between a pixel and a signature is calculated by the following relationship where the user chooses the degree to which color differences (ΔC) and brightness differences (ΔB) are to be weighted (WCLR and WBRT respectively):

$$D = \sqrt{WCLR \cdot (\Delta C)^2 + WBRT \cdot (\Delta B)^2}$$

where $WBRT + WCLR = 1$.

If the distance D is less than the user-specified value (DELMAX), then the unknown pixel will be classified as belonging to the surface type associated with that signature.

A four-dimensional classification volume is described about each signature. The shape and orientation of the volume changes depending on the values of WBRT, WCLR, and DELMAX, but is generalized as a distorted hyper-ellipsoid inscribed within a truncated cone.

The initial step in the classification procedure was the selection of 22 control areas in the Estuary. These areas measure 6 x 6 pixels and were chosen in east-west pairs at 11 latitudes (Figure 1). T-tests were performed on the differences among the means of all 22 areas. A t-statistic of 1.692 or greater (95% confidence) was taken to indicate a significant difference between

two control areas. Two control areas were chosen on each side of the river (E1 and E9 on the east and W1 and W9 on the west, Figure 1) such that they were similar to most of the other control areas on the same side of the river and different from most of the control areas on the other side of the river. Reference signatures for western and eastern water were calculated by combining the appropriate two control areas for each type. Landsat MSS Bands 4 and 5 alone were sufficient to differentiate the western and eastern reference signatures; therefore, Bands 6 and 7 were discarded, and a two-dimensional classification was performed. The reference signatures ($\text{mW.cm}^{-2}.\text{sr}^{-1}.\text{ch}^{-1}$) are listed below:

	B4	B5
western	.446	.229
eastern	.394	.191

The optimum values of WBRT, WCLR, and DELMAX were chosen for each reference signature as the lowest value of DELMAX and the value of WBRT and WCLR that minimized the sum of the errors of omission and commission. These values are listed below and the classification areas that they describe are shown in Figure 3 along with a B4-B5 plot of the pixels in the two reference signature groups.

	DELMAX	WBRT	WCLR
western	0.055	0.2	0.8
eastern	0.055	0.5	0.5

Each pixel in the study area was subsequently classified as "western", "eastern", or "neither". The classification is order dependent; once a pixel is successfully tested for classification with one signature, it is not tested against other signatures. However, this was not a problem, because the overall pattern and classification showed little difference whether "eastern" or "western" water was classified first. That is, there are very few pixels whose spectral characteristics placed them in both categories. Further, very few pixels in the Estuary fall in neither classification area and are unclassified. Errors of omission and commission are given for the reference signature control areas in Figure 3. A copy of the printout of the pixel by pixel classification of a representative portion of the river is shown in Figure 4. The boundary between "eastern" and "western" water is interpreted as the point on each row where "eastern" pixels begin to dominate over "western" pixels. Unclassified pixels and classifications obviously influenced by "sixth row striping" are ignored.

5. DISCUSSION OF THE LANDSAT CLASSIFICATION

The interpreted classification map for the whole study area (Figure 1) confirms the existence of a lateral gradient in the surface spectral properties of the Hudson River Estuary. The Landsat data clearly distinguish and map these gradients on a scale at least as small as one half kilometer. A t-test comparing the means of the reflected radiance values of the combined (11 x 36) eastern and combined (11 x 36) western control area pixels showed them to be significantly different for both Bands 4 and 5 with t-statistics of 12.44 and 20.69 respectively. These are significant at greater than 99.95% confidence. Several possible explanations for this lateral gradient were mentioned earlier.

Figure 5 shows a bathymetric cross section of the Estuary with the corresponding B4 and B5 values of Landsat data plotted. While the brighter Landsat spectral values occur on the west where the river is shallow, it is clear that the Landsat spectral values do not increase as the river shallows on the eastern shore. This non-correlation of bathymetry and reflected radiance is also borne out on other cross sections of the Estuary not reproduced here.

The spectral properties of four freshwater reservoirs near the shore of the Hudson were also studied; and three of these freshwater reservoirs have spectral characteristics consistent with the more saline eastern river water. One of the reservoirs, Lake Tappan, had distinctly brighter, western water spectral characteristics. The water in the Lake Tappan reservoir was very silty because of ongoing construction at the time of the Landsat overpass. It appears, therefore, that salinity is not the controlling factor in the spectral differences observed laterally across the Hudson, but that turbidity may control the spectral differences. This observation is consistent with other studies which were cited above and report increased reflected radiance values, particularly in Band 5, with increased turbidity.

There is no lateral contrast of Landsat spectral properties in the Estuary from 57th St. in Manhattan south to the lower portion of the Upper Bay. In this region, water with spectral properties of "western" water predominated on both sides of the Estuary. This may be due to the fact that the Landsat overpass occurred at the time of slack following the ebb tide, which coincides with low tide. The tidal current chart (Figure 6) shows that this is the end of the 6-hour period during which highly turbid East River and Kill Van Kull water and sewage effluent from lower Manhattan have been flowing into both sides of the Estuary. Specific locations of major sewage discharge into the Estuary are given by Simpson et al., (1975).

Near the Verrazano Narrows, where very strong tidal currents and intense turbulence exist, the pixels are about evenly distributed between "western" and "eastern" classifications, with no discernable spatial clustering or patterns of either classification.

6. CONCLUSION

This analysis of the Landsat data leads us to conclude that there is a relatively strong downstream flow on the west side of the river, and that this western water is more turbid and less saline than the eastern water. On the east side of the river, there is a weaker downstream flow, with saline water making its way farther upstream on the eastern shoreline. It is clear that differences in the spectral properties of the Landsat digital data can be mapped and used as indicators of circulation and dispersion in the Hudson Estuary.

ACKNOWLEDGEMENTS

The study was supported by NASA Grant NSG 5014. The computer used in the study is located at the Goddard Institute for Space Studies (GISS) in New York City and accessed by a remote terminal at Dartmouth College. The authors benefited from the cooperation and help of members of the GISS staff, in particular Stephen Ungar. D. Weiss of the City University of New York and the crew of the R.V. Commonwealth provided salinity data. Emily Bryant, David Teplow, and Betty Stroock of Dartmouth College helped with the Landsat data interpretation. John Hughes of Dartmouth College provided important contributions to the statistical treatment of the data. We also benefited from discussions with Charles Officer of Dartmouth College.

REFERENCES

- Johnson, R.W., 1978, Mapping of chlorophyll *a* distributions in coastal zones: *Photogramm. Eng. and Remote Sensing*, v. 44, p. 617-624.
- _____, and G.S. Bahn, 1977, Quantitative analysis of aircraft multispectral-scanner data and mapping of water-quality parameters in the James River in Virginia: *NASA Tech. Paper*, 1021, 31 pp.
- Khorram, S., 1979, Remote sensing analysis of water quality in the San Francisco Bay Delta: *Proc. 13th Int. Symp. Rem. Sensing of Environ.*, p. 1591-1601.
- Klemas, V. and D.F. Polis, 1976, Remote sensing of estuarine fronts and their effects on oil slicks: *Paper No. CMS-RANN-4-76*, College of Marine Studies, Univ. of Delaware, 48 pp.
- Maness, L.V. and P.W. Mausel, 1979, Slat wedge delineation in the Pamlico Estuary, N.C.: abstract in *Prof. Paper No. 11, Dept. Geog. and Geol., Indiana State Univ.*, p. 52-53.
- Merry, C.J., H.L. McKim, S. Cooper, and S.G. Ungar, 1977, Preliminary analysis of water equivalent/snow characteristics using Landsat digital processing techniques: *Proceedings of 1977 Eastern Snow Conference*, Beltsville, Ontario, Canada.
- Mausel, P.W., S.J. Stadler, L.V. Maness, and W.W. Birkhead, 1979, Machine processing of satellite multispectral data for coastal zone ecological analysis: in *Prof. Paper No. 11, Dept. Geog. and Geol., Indiana State Univ.*, p. 10-22.
- Pesmentier, E.S., 1977, Applications of remote sensing technology and information systems to coastal zone management: in *Earth Observation Systems for Resource Management and Environmental Control*, ed. by D.J. Clough and L.W. Morley, Plenum Pub. Co., p. 353-363.
- _____, and J.W. Rachlin, 1976, Distribution of salinity and temperature in the Hudson Estuary: *J. Phys. Oceanogr.*, v. 6, p. 775-777.
- _____, and J. Raymont, 1979, Variations of longitudinal diffusivity in the Hudson Estuary. *Estuar. and Coastal Mar. Sci.*, v. 6, p. 555-564.
- Rouse, L.J., and J.M. Coleman, 1976, Circulation observations in the Louisiana Bight using Landsat imagery: *Remote Sensing of Environment*, v. 5, 55-66.
- Simpson, H.J., D.E. Hammond, B.L. Deck, and S.C. Williams, 1975, Nutrient budgets in the Hudson River Estuary: in *Marine Chemistry in the Coastal Environment*, ed. by T.M. Church, American Chemical Society Symposium Series No. 18, p. 618-635.

ORIGINAL PAGE IS
OF POOR QUALITY

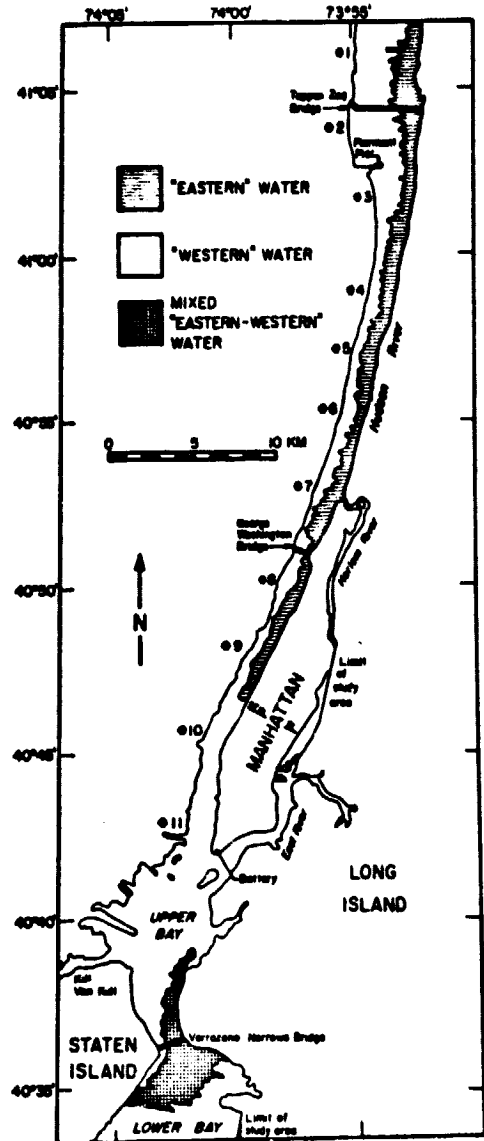


Figure 1.
Lower Hudson River Estuary

Interpretation of Landsat digital data for Lower Hudson River Estuary. Zones of generally "eastern", "western", and "mixed" water are identified. Locations of control areas at eleven different latitudes are indicated as #1 through #11. At each latitude, a pair of control areas were chosen, one on the east and one on the west (for example, E1 and W1 respectively).

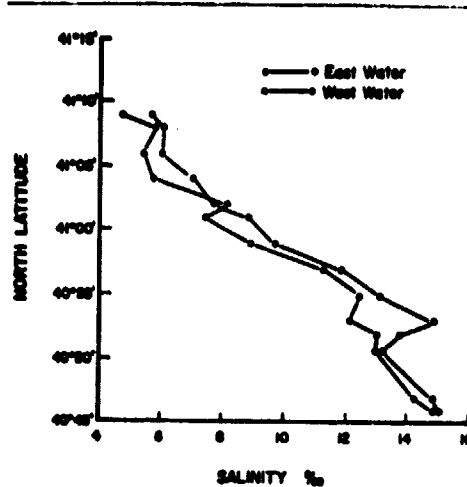


Figure 2. Salinity Data

Salinity as a function of latitude in the Hudson Estuary. At each latitude, salinities for water on the eastern and western half of the Estuary are plotted individually.

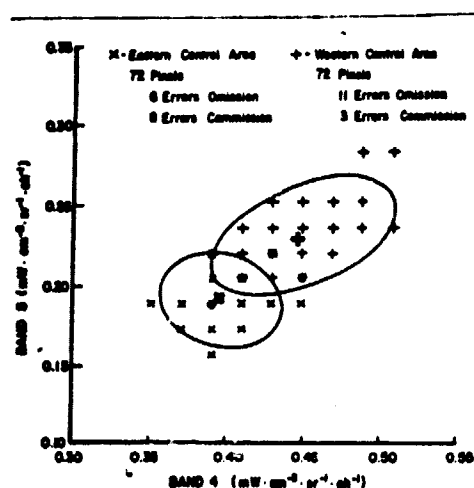


Figure 3. B4-B5 Pixel Plot

Plot of B4-B5 reflected radiance values for pixels in the eastern (x) and western (+) reference signature control areas. Values occurring in both control areas are shown with an x. The means of each control area are shown by the appropriate bold lined symbol. Many values represent more than one pixel but these are not indicated. The classification area for each control area is outlined.

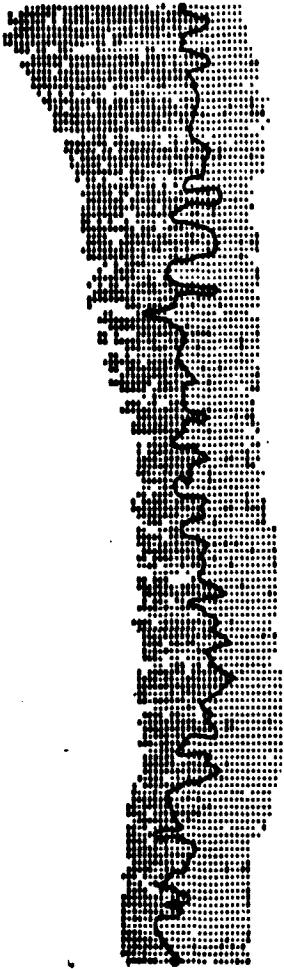


Figure 4. Classification

Pixel by pixel classification of a 10.3 km stretch of the Estuary between about 40°56' and 41°02' north latitude. @ represents "western" water, * represents "eastern" water, and blanks represent "neither" (unclassified). The interpreted boundary between western and eastern water is drawn in.

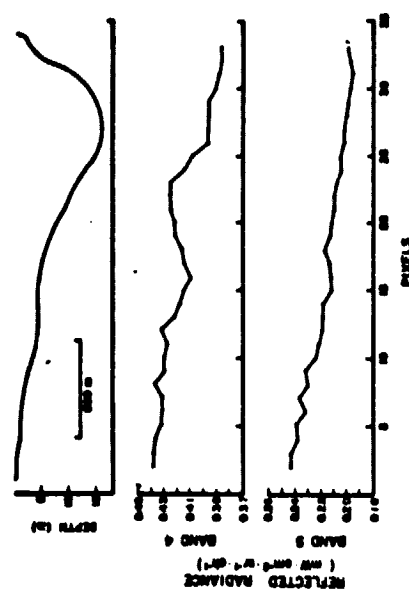
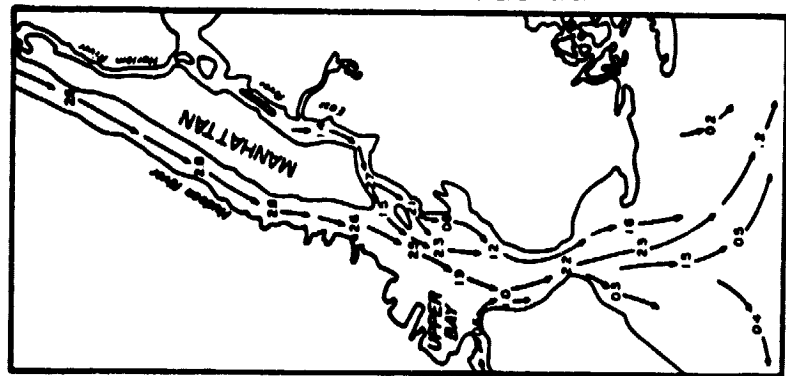


Figure 5. Cross Section

Bathymetry and Landsat B4 and B5 reflected radiance values for an east-west cross section of the Estuary at the latitude of control area #3 (Figure 1). The reflected radiance values are smoothed by averaging nine pixels, three pixels in each of three adjacent rows of Landsat data.

Figure 6. Tidal Current Chart

Tidal current chart of the Hudson River Estuary three hours before the time of the Landsat overpass on 27 October, 1972 (from U.S. Coast and Geodetic Survey Spec. Pub. #152, Tidal Current Charts, New York Harbor, 1928).

Remote Detection of Geobotanical Anomalies
Related to Porphyry Copper Mineralization

by

Richard W. Birnie and
Joseph R. Francica

Department of Earth Sciences
Dartmouth College
Hanover, NH 03755

(Revised)
(Submitted to Economic Geology) Encl 6
June 1980

ABSTRACT

Visible and near infrared (450-1000 nm) reflected radiance spectra of the ground cover vegetation were measured at the Mesatchee Creek porphyry copper prospect in Washington. The reflected radiance data are integrated over 400 m² surfaces of a forest predominated by Douglas fir with lesser amounts of western larch. Analysis of the reflected radiance data indicates that the spectra from within the pyrite halo of the deposit have anomalously high reflected radiance values at 565 nm and low reflected radiance values at 465 nm. Six flight lines were flown on each of two days. Taking one flight line from the first day's data as the control line, individual spectra with a 565 nm/465 nm reflected radiance ratio value greater than 1.7 fall predominantly within the pyrite halo. When this threshold value is applied to all flight lines from the first day, 36.8% of the spectra within the pyrite halo and 5.4% of the spectra outside the pyrite halo are classified as anomalous. The zone of mineralization is clearly defined by the cluster of anomalous spectra. There is an 87% probability of an anomalous spectrum lying within the mineralized zone. The same technique was applied to the second day's data. The threshold ratio value was optimized at 1.6 and the resultant probability of an anomalous spectrum lying within the mineralized zone is then 92%. Higher cutoffs improve the probability of an anomalous spectrum falling in the mineralized zone; but fewer spectra are classified as anomalous, and the extent of the

mineralized zone is not as well defined. The geobotanical anomaly correlates with the pyrite halo and is not preferentially concentrated within the high Cu soil geochemical zones. Comparison with results obtained in lodgepole pine at Heddleston, Montana, show that different vegetation types manifest geobotanical anomalies in different spectral regions.

JOHN M. HUGHES
WINTER TERM, 1980

The following computer programs were written for use with LANDSAT digital data: MATT, MATT1, TTEST, and BPLOT1. These programs are stored in R.W. Birnie's user number on the Dartmouth Computer. Printouts of the programs are attached. A brief description of each follows.

MATT: Performs a student's T test on Control Area files (Pixel X Band files). Outputs data in a file X file matrix, giving two places to right of decimal. Output represents confidence levels for the null hypothesis.

MATT1: Same as above program, but prints out confidence levels in integer values. This enables user to print out up to a 24 X 24 matrix of control areas.

TTEST: Program performs a t-test on only two different Pixel X Band files. Gives confidence levels for all four bands between two files.

BPLOT1: Plotting program designed for use with Landsat MSS bands. The program asks for one or two files containing a Pixel X Band matrix and plots a point for each pixel in two band coordinates. Also calculates mean for each group of pixels, and draws Giss volume for each file if desired.

PGK

40



Dartmouth College HANOVER · NEW HAMPSHIRE · 03755

Department of Earth Sciences · TEL. (603) 646-2373

April 23, 1980

COPY

Trip Report

To: Mt. St. Helens, Vancouver, Washington

On March 28, we flew to Portland, Oregon to witness the eruption of Mt. St. Helens, measure the SO₂ output with the COSPEC, and obtain samples of fresh ash for further study. We secured the use of a Navajo Chieftain twin engine plane, courtesy of NBC News, for airborne use of the COSPEC.

We had minor trouble with the sensitivity of the instrument but were able to make 27 traverses under 11 different eruption plumes over the ensuing 7 days. SO₂ output averaged approximately 30 tons per day. One fresh dry sample of ash was obtained. We returned to Hanover on April 6, 1980.

A manuscript, copy attached, was prepared, reviewing the scientific results of our visit and the subsequent visit by Larry Malinconico. It has been submitted to Science.

The COSPEC, chart recorder, and tripod have been left in Vancouver, Washington. The COSPEC will be land carried to Denver before May 23. The accessories will be shipped to Dartmouth. David Johnston, of the USGS, now in Vancouver, WA., is in charge of our instrument at this time.

Richard E. Stoiber
Stanley Williams

cc: Dick Stoiber
Stan Williams
Phil Krueger

Encl 8

Trip Report

To: Mt. St. Helens Volcano
Vancouver, Washington.

On April 9, 1980 I travel^f to Vancouver, Washington with the COSPEC. For the next three days I worked with personnel from the U.S.G.S. measuring the SO₂ flux from Mt. St. Helens volcano. Several small eruptions were measured with flux rates averaging 30 t day⁻¹. On the 11th and 12th a static plume was measured and had a flux of 3 t day⁻¹.

I also instructed David Johnston and Tom Casadevall of the U.S.G.S. on the use and care of the COSPEC as they will be continuing the SO₂ monitoring of the volcano.

On the 12th a sample of ash was collected from the summit of the volcano for leachate analysis.

I returned to Hanover on April 13, 1980.

Lawrence L. Malinconico
April 17, 1980

Enc 9

TRIP REPORT**MT. ST. HELENS AND NCAR REVIEW MEETING**

Stan Williams and Dick Stoiber spent May 18-22 and May 25-26 at Vancouver, Washington. The purpose of the trip was to measure SO₂ after the big eruption of 18 May with our Cospec which we had left with Dave Johnston of the USGS. He was making measurements without benefit of airplane support. Since we knew NBC (Barrington) was at St. Helens we expected to be able to use our Cospec in a plane he would provide.

On arrival in Vancouver WA. it was discovered that Dave Johnston had been killed by the direct blast of 18 May and our entire instrument package was destroyed. The USGS was expecting delivery of a new Cospec which was lost in transit. Upon arrival in Vancouver we turned our attention to tracing the instrument, expediting its delivery, arranging to send the Dartmouth chart recorder to Vancouver, and finding a portable 14 volt power source. We found the Cospec which had been broken in transit, and repaired it.

We left for our NCAR meeting in Denver late Thursday by night flight from Portland, Ore. We went with Bill Rose, Irving Friedman, Leslie Zinser and Dick Cadle at NCAR. Publication and presentation of results of the Feb. 1980 volcanic plume flights in Guat. were discussed with the following tentative plan:

Abstracts for the Dec. 8-12 AGU in San Francisco as

Enc 1D

THE PAPER IS
A GOOD QUALITY
follows:

- 1) Dispersion of SO_2 in volcanic plumes, Stoiber, Williams, and Malinconico
- 2) SO_2 and isotopes at Pacaya and Santiaguito, Friedman, Williams, Malinconico
- 3) SO_2 change through time at several volcanoes, Stoiber, Malinconico

Publication of complete papers at near this date.

We met with Barry Huebert of Colorado College on Saturday to discuss filters used to obtain HCl/SO_4 ratio data. He will cooperate on gas work we intend to do in Nicaragua summer 1980 and written 1981.

We left for Portland by night flight from Denver on Saturday, May 24. We monitored SO_2 from the air Sunday May 25. The SO_2 was being emitted from a medium sized eruption, which occurred near midday at a $2400 + \text{day}^{-1}$ rate. Data for further airborne measurements made while the volcano was relatively quiet the morning of May 26 has not been processed yet.

We returned to Hanover Monday noon arriving early Tues. AM!

In summary: we find that SO_2 was now emitted at normal rates in the Mt. St. Helens eruption. we found the USGS instrument and put together an operative instrument package.

We encouraged the USGS to use their instrument in the airborne mode and we think they will. We left our chart recorder with them til theirs is found (lost in transit) so measurements can be made. We collected an extensive suite of fresh ash for analysis in Hanover. We made a valuable contact with Barry Huebert with respect to future gas work.

RE Stoiber

Trip Report: Mount St. Helens
July 2 - July 9, 1980

During the period July 2 through July 9, 1980 monitoring of the SO_2 gas emission from Mt. St. Helens volcano was continued.

I arrived in Vancouver, Washington on July 2. However, heavy rains did not allow monitoring until the afternoon of July 5. SO_2 measurements were also made on July 6, 8 and 9. The results are included on a separate page. The range of daily averages (1600 to 2600 $\pm \text{d}''$) for this period is higher than the $1000 \pm \text{d}''$ determined by Casadevall for the previous weeks. This could be due to several reasons. The most probable explanation is that the very good weather during the period allowed us to get totally under the plume. A second explanation is that there is a real increase perhaps associated with the tidal maximum which occurred on July 10. A final explanation is that there was a real increase due to increasing volatile pressure in the magma body. If this is true and the pressure is building it could signify the possibility of another eruption.

L. Malinconico

Encl 11

SO_2 data

Mt. St. Helens

July 2 - July 9, 1980

July 5: 2280, 2980, 3020, 2200

$$\bar{x} = 2620 \pm 440 \text{ d}^{-1}$$

July 6: 1379, 1807 (7000' altitude) $\bar{x} = 1590 \pm \text{d}^{-1}$

1703, 1832 (6000' altitude) $\bar{x} = 1770 \pm \text{d}^{-1}$

July 8: 1455, 2840, 1800, 2180, 1920, 3040, 1500

$$\bar{x} = 2100 \pm \text{d}^{-1}$$

July 9: 1540, 1660, 1600, 1940, 1980, 1650, 1840

1230, 1090, 1280

$$\bar{x} = 1580 \pm \text{d}^{-1}$$

SO₂ EMISSIONS
ACTIVITY